Opto-mechanical analysis and design tool for adaptive X-ray optics

Gregory Michels, Victor Genberg
Sigmadyne, Inc. 803 West Ave, Rochester, NY 14611
michels@sigmadyne.com

ABSTRACT

Adaptive X-ray optics offer significant potential for new optical systems. An analysis and design tool for the opto-mechanical design of adaptive X-ray optics is presented. The key issues addressed are:

1) The processing of finite element nodal displacements for optical surface characterization is illustrated.

2) The fitting of Fourier-Legendre polynomials to the radial sag or surface normal displacements of near cylindrical optics is presented.

3) The use of 2D Legendre polynomials are presented as an alternative representation of mechanical displacements.

4) The analysis of adaptive X-ray optics requires the solution of actuator strokes required to minimize surface RMS. Issues include stroke limits and surface slope error minimization.

5) The number and placement of actuators can be optimized by using an embedded genetic selection algorithm.

6) The mirror structure and mounts may be optimized to minimize the adaptively corrected surface error while still satisfying all structural requirements.

7) The implementation of a Monte Carlo technique to predict the impact of random factors in the system such as actuator resolution or mount strain forces.

Keywords: finite element, Fourier-Legendre, Legendre, adaptive, optimization, opto-mechanic, X-ray

1. INTRODUCTION

The design challenges to develop grazing incidence X-ray optics for modern systems such as the International X-Ray Observatory (IXO) are well known to be daunting.[1] The ability to characterize results from mechanical analysis software tools and to transfer those characterizations to optical analysis software tools was a valuable asset to the design development of the Chandra X-Ray Observatory.[2] A flow chart of this analysis process is shown in Figure 1. SigFit is a commercial software tool from Sigmadyne which is used in the integrated opto-mechanical analysis of optical systems as shown in Figure 1.[3,4] While SigFit has been in practice for the development of normal incidence optics, recent enhancements have been added to allow analysis of grazing incidence optics such as those used in X-ray astronomy. This paper discusses the methods and capabilities implemented in SigFit specifically with regard to passive and adaptively controlled grazing incidence optics.

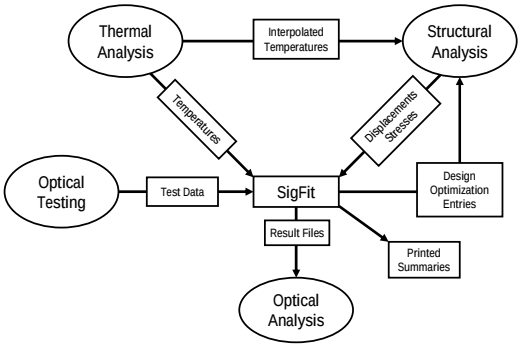

Figure 1. Opto-mechanic analysis flow

2. PROCESSING OF FINITE ELEMENT DISPLACEMENTS

In order to describe the deformed shape of a cylindrical optic as predicted by finite element analysis (FEA), the nodal displacement vectors must be processed into a form useable to describe the deformed shape. Figure 2 illustrates a deformed cylindrical optic with an undeformed node P and a corresponding displaced node P' as predicted by analysis such as FEA. In addition, the normal deformation and radial deformations of the original location P are shown as labeled. Notice that the displacement vector given by **PP'** is neither the normal nor the radial sag displacement of the deformed optic. The desired normal or radial sag deformations, which are the deformations commonly employed for the purposes of describing the deformed shape of the optical surface, must be computed from the displacement vector given by **PP'**.

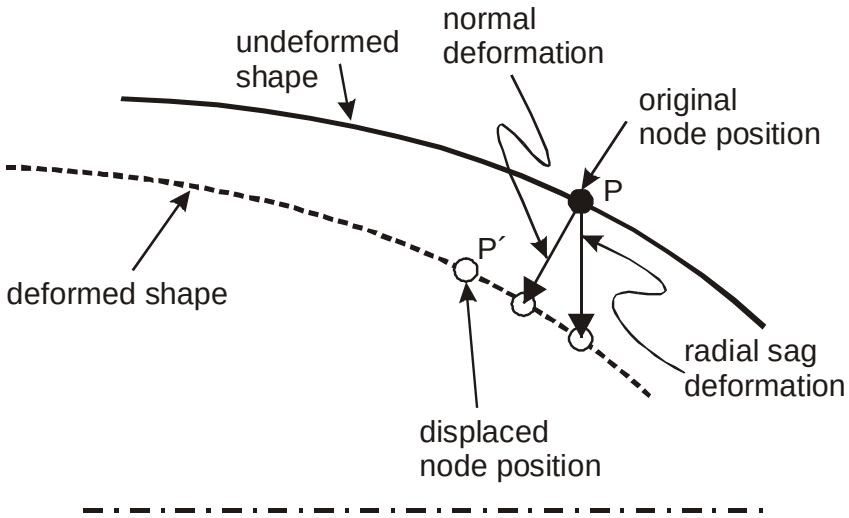

Figure 2. Illustration of normal and radial deformation relative to the displaced node position as represented by FEA results.

It can be shown that the normal deformation of the optic can be approximated to first order by simply taking the component of the FEA nodal displacement vector in the direction of the surface normal. The first order approximation of the radial sag deformation is somewhat more complicated as it involves the first derivative of the radial sag of the surface prescription with respect to the axial coordinate. The process of converting the FEA nodal displacement into the radial sag deformation is called *axial correction* as it incorporates the effect of axial displacement on the radial sag. While the method described in Figure 2 ignores the effect of azimuthal displacements, a generalization can be made to account for all three nodal translations predicted by FEA. In the case of axisymmetric optics, the effect of azimuthal displacement on the radial sag is generally of lower order than the effect of axial displacements.

The need for axial correction is shown in the following example where an optic with a kinematic mount midway between the upper and lower edges is subjected to an isothermal temperature increase. The low order deformation terms of average radial growth and cone have been subtracted. The most significant remaining deformation of barrel shows an opposite sign with and without axial correction and is shown in Figure 3. This is illustrating that axial displacement causes an effective radial displacement and neglecting it leads to erroneous results. The correction is, therefore, especially important with thermoelastic loads, which tend to have high axial growth compared to radial growth due to the nature of the geometry.

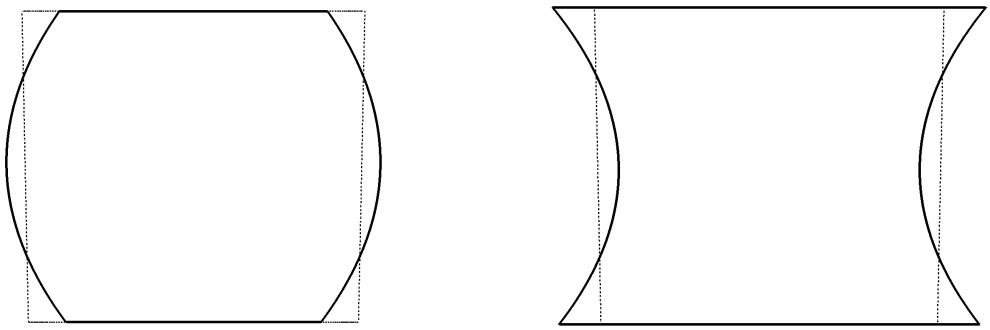

(a) (b)

Figure 3. Deformed plots of only radial deformation illustrating barrel distortion (a) without axial correction and (b) with axial correction.

3. FOURIER-LEGENDRE POLYNOMIALS

The use of Fourier-Legendre polynomials[5] is a common means to quantify the deformed shape of a cylindrical optic. Fourier-Legendre polynomials are defined by Equation 1 where *n* is the axial wave number and *m* is the circumferential wave number.

$$f(z,\Theta) = \sum_{n=0}^{N}\sum_{m=0}^{M} P_n(z)\left[A_{nm}\cos(m\Theta) + B_{nm}\sin(m\Theta)\right] \tag{1a}$$

$$P_n(z) = \sum_{k=0}^{K}(-1)^k \frac{(2n-2k)!}{2^n k!(n-k)!(n-2)!} z^{n-2k} \tag{1b}$$

Plots of several low-order polynomials appear in Appendix A. Fourier-Legendre polynomials (FLG) are similar to Zernike polynomials (ZRN) in several ways.

1. *n* = axial wave number in FLG, *n* = radial wave number in ZRN.
2. *m* = radial wave number in both FLG and ZRN.
3. Both FLG and ZRN form an orthogonal set. FLG are orthogonal over the full cylindrical aperture of -1 < z < +1 while ZRN are orthogonal over a circle of unit radius.
4. Both FLG and ZRN may be normalized to unit amplitude or unit RMS.
5. Both may be fit to normal or sag displacement. Sag for FLG is radial displacement while sag displacement for ZRN is axial displacement. See Figure 2 for an illustration of radial sag displacement.

The coefficients of the Fourier-Legendre polynomial fit may then be used as input to an optical analysis model to allow optical performance predictions of the optic.

4. LEGENDRE POLYNOMIALS FOR SEGMENTED OPTICS

For segmented cylindrical optics, the deformation in each segment may be independent of other panels. Polynomials continuous over the full cylinder, such as FLG, will not represent a good fit to deformation data as they will not be able to capture the discontinuities introduced by the separate segments. Legendre polynomials[5] (LEG), on the other hand, may be defined over a single cylindrical segment. Plots of low order LEG polynomials appear in Appendix B. LEG polynomials are similar to XY polynomials for conventional optics, except that:

1. LEG form an orthogonal set, whereas XY do not.
2. LEG may have an independent normalization for each domain variable . XY have a single normalization used for both domain variables.

When applied to grazing incidence optics, LEG are fit with respect to the axial (Z) and circumferential (Θ) directions with an independent normalization of each. The user may choose to fit surface normal (*s* = *dn*) or radial sag (*s* = *dr*) deformation.

$$s = \sum_{n=0}^{N}\sum_{m=0}^{M} c_{nm} P_n(z) P_m(\Theta) \tag{2a}$$

$$P_n(z) = \sum_{k=0}^{K} (-1)^k \frac{(2n-2k)!}{2^n k!(n-k)!(n-2)!} z^{n-2k} \qquad P_n(\Theta) = \sum_{k=0}^{K} (-1)^k \frac{(2m-2k)!}{2^m k!(m-k)!(m-2)!} \Theta^{m-2k} \tag{2b}$$

In Figure 4 a segmented optic and a continuous optic with a circumferential gradient are compared. When the continuous optic is fit with Fourier-Legendre polynomials through order (*n*=6, *m*=6), 99.7% of deformation is represented. If the same fit is applied to the segmented optic, only 94.4% of the deformation is represented, missing 5.6%. When Legendre polynomials through order (*n*=6, *m*=6) are applied independently to each segment, the fit represents 99.98% of the deformation, missing only 0.02%.

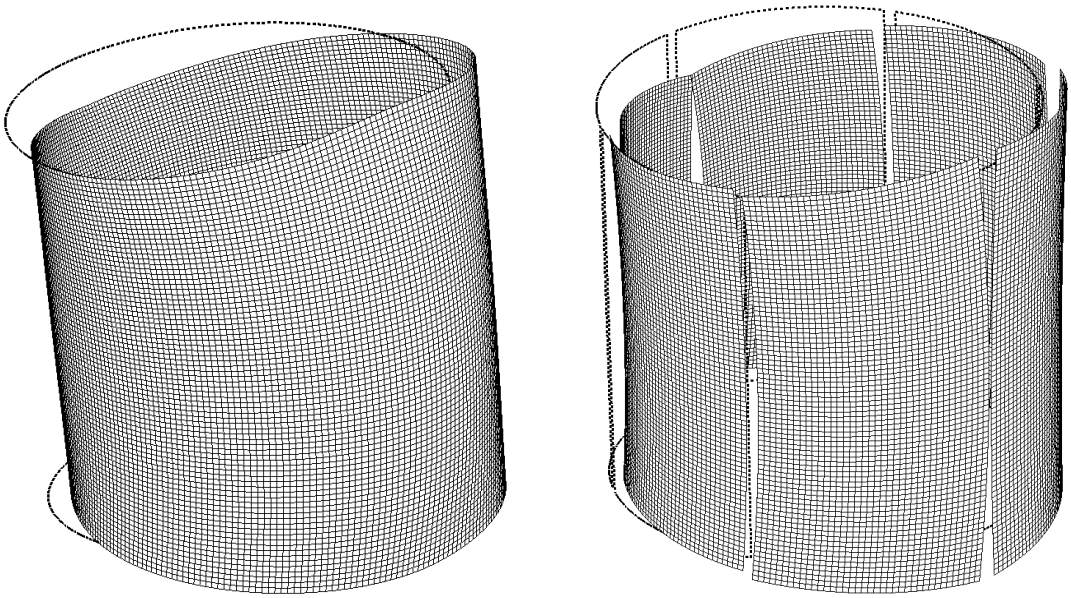

(a) (b)

Figure 4. Deformation due to circumferential thermal gradient for (a) continuous optic and (b) a 6-panel segmented optic.

The coefficients of the Legendre polynomial fit may then be used as input to an optical analysis model to allow optical performance predictions of the optic.

5. ANALYSIS OF ADAPTIVE X-RAY OPTICS

SigFit's adaptive analysis capability will solve for the actuator amplitudes required to minimize the surface error.[6] Actuator influence functions may be supplied through FEA results in the same manner as the disturbances to be corrected. Actuators included in adaptive control simulation may, therefore, be force or displacement type, either external or embedded within the optic or any influence that may be simulated in FEA and is linearly related to its controlling input, *A*. The actuator inputs for best correction of the optical surface are computed by minimization of the mean square error function defined as,

$$E = \sum_{i=1}^{N} w_i \left(ds'_i - \sum_{j=1}^{M} A_j f_{ji} \right)^2 \tag{3}$$

where,

N = the number of nodes,
w_i = weighting coefficient of node i,
M = the number of actuator influence functions,
ds'_i = surface deformation at node i, (radial or normal)
A_j = actuator input for actuator influence function j,
f_{ji} = surface deformation of actuator influence function j at node i.

Taking partial derivatives of E with respect to each actuator input and setting each equal to zero leads to a linear system of M equations for M unknowns,

$$[H]\{C\} = \{F\}, \tag{4a}$$

$$H_{jk} = \sum_i w_i f_{ji} f_{ki} , \tag{4b}$$

$$F_k = \sum_i w_i ds'_i \, f_{ki} , \tag{4c}$$

which allows for computation of the actuator inputs which minimize the error E.

SigFit also offers an option to include slopes along with sag or surface normal translations in the minimization of surface RMS. The user input is a slope fraction, c, whose value ranges from 0.0 (no slopes included) to 1.0 (no translations included). Since displacements and slopes are in different units, slopes must be converted to displacement units. To convert radians to displacement units, SigFit multiplies the slopes by the average node spacing, L. In SigFit, L is calculated from the optic surface area, a, and the number of nodes on the surface, N.

$$L = \sqrt{\frac{a}{N}} \tag{5}$$

Let Θ_i = x-slope at node i and Φ_i = y-slope at node i, then the combined error to be minimized is:

$$E = (1-c)\sum_{i=1}^{N} w_i \left(ds'_i - \sum_{j=1}^{M} A_j f_{ji} \right)^2 + (c)(L)\sum_{i=1}^{N} w_i \left(d\Theta'_i - \sum_{j=1}^{M} A_j \Theta_{ji} \right)^2 + (c)(L)\sum_{i=1}^{N} w_i \left(d\Phi'_i - \sum_{j=1}^{M} A_j \Phi_{ji} \right)^2 \tag{6}$$

Note that using slope data in the fit is only valid if the FE model predicts meaningful slope data. Solid finite element models, for example, generally do not generate slope data. Shell elements are often required to create valid slope output.

In adaptive analysis, the user may specify limits on actuator motion or force level. If selected, SigFit will find the best corrected surface RMS within the allowable actuator limits. SigFit first finds the unbounded solution according to the method presented above. Then, if any of the corrected cases violates the actuator limits, those cases will be resolved with nonlinear programming techniques using the imposed limits.

For orbiting telescopes, actuators that may fail during operation are not easily repaired, if possible at all. Actuator failure is easily analyzed in SigFit by deleting the failed actuator's influence function from the solution set.

6. ACTUATOR PLACEMENT OPTIMIZATION

As part of an adaptive control analysis in SigFit, the user may optionally conduct actuator placement optimization.[7] When actuator placement optimization is selected, SigFit will invoke a genetic optimization algorithm[8] to find the set of actuators chosen from a candidate actuator set which provides the lowest corrected surface RMS error.

The overall flow of this optimization algorithm is shown in Figure 5. SigFit begins by randomly selecting a number of actuator layouts each containing the number of actuators specified by the user. This randomly selected set of layouts is called the initial population. The corrected surfaces associated with these actuator layouts are evaluated. Three operations are then performed on this initial population: mating selection, crossover, and mutation. The outcome of these three operations will result in a new population called a generation. This new population is then evaluated to find each actuator layout's corrected surface error as was done for the initial population. As the optimization loops through generations the corrected surface error of each member of each new generation is compared to the lowest corrected surface error of all prior generations. When a more superior design is not found for a user specifiable number of successive generations, the optimization is terminated and the best actuator layout is passed to adaptive control simulation for final analysis.

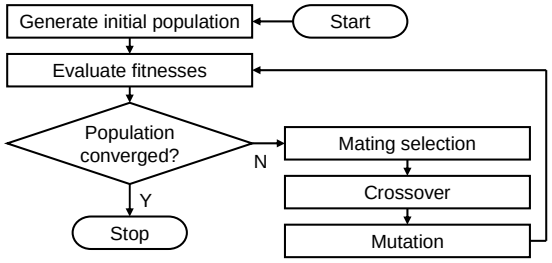

Figure 5. Flowchart of genetic optimization algorithm.

Specifying candidate actuators in groups allows the user to enforce symmetry in the actuator layouts considered by the optimizer.

As an example the genetic optimizer was applied to a single segment of the AXAF-like model above with two load cases of axial gradient and a circumferential thermal gradient. A full set of 200 actuators was distributed evenly as candidate actuators as shown in Figure 6.

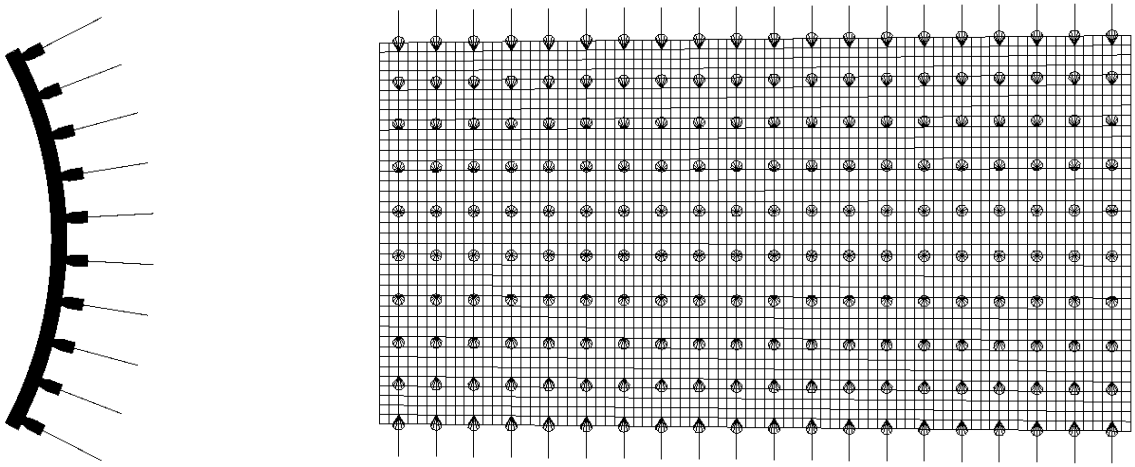

(a) (b)

Figure 6. Candidate actuator locations on 60 degree cylindrical mirror segment.

Using the actuator placement optimization in SigFit the optimum sets of 20, 40, 60 and 80 actuators were found. A plot of the residual error verses the number of actuators is given in Figure 7.

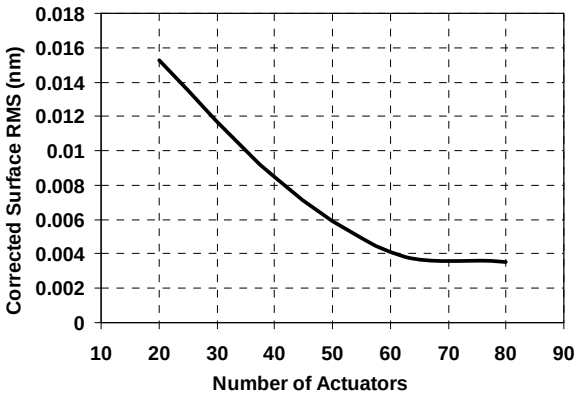

Figure 7. Plot of residual error verses number of actuators.

The locations of the actuators in the optimum actuator layouts for the 20-actuator case and the 40-actuator case are shown in Figure 8. Notice that the set of actuators found by the optimizer results in force pairs creating effective edge moments to control the bending caused by the thermal gradients. This corrective loading is consistent with fundamental elasticity theory.

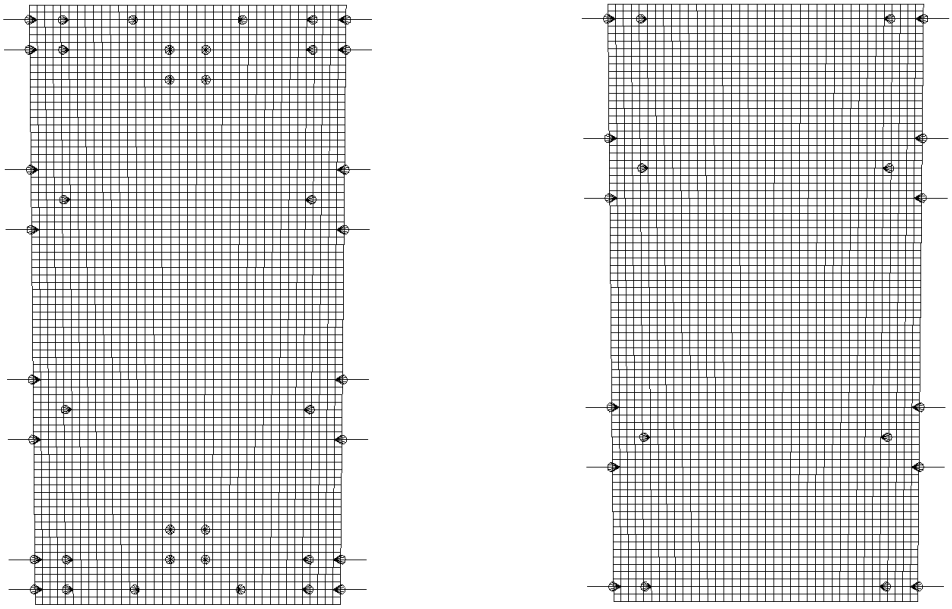

(a) (b)

Figure 8. Optimum actuator sets for (a) 40 actuators and (b) 20 actuators.

7. STRUCTURAL OPTIMIZATION

SigFit offers two methods for structural optimization using optical measures as response quantities to limit or minimize. In one method, SigFit writes NASTRAN[a] format DRESP2 equations in bulk data format. These equations represent surface distortion RMS and peak-to-valley response with the users choice of rigid-body motion or any polynomials subtracted. For example, the user may wish to create a mirror design which minimizes surface RMS after rigid-body motion and power have been removed, and still satisfy all other mechanical requirements.[6]

[a] NASTRAN is a registered trademark of the National Aeronautics and Space Administration.

In a second method, SigFit is called as an external subroutine through the DRESP3 feature in MD Nastran[b]. In this approach, SigFit can calculate and return any of the available responses as a quantity for optimization. A common application of the DRESP3 generation feature is to optimize structural design to minimize the corrected surface of an adaptive optic.[9]

8. VIBRATION ANALYSIS

Even though commercial FE programs offer a full suite of vibration analyses, their output is not geared towards opto-mechanical analysis. If a random response analysis is run in an FE program, the resulting output is the 1-sigma response at each node. This is an amplitude response with no phasing information. Therefore, the results do not distinguish between behaviors that have very different effects on optical performance. An example of such behaviors is shown in Figure 9 where piston motion and a sinusoidal deformation cannot be distinguished from nodal random response results.

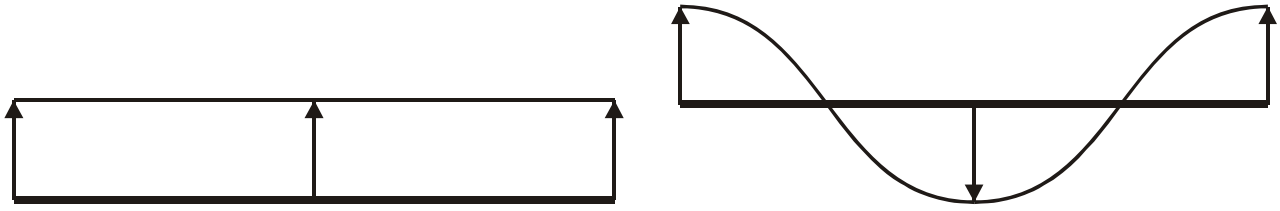

Figure 9. The surface RMS of the piston motion shown in (a) is equal to the surface RMS of the elastic motion shown in (b) when performing random response within a commercial finite element program, which is unable to decompose such specific behaviors.

SigFit, however, has a vibration analysis capability to rectify this shortcoming. In SigFit, the modal eigenvectors of each surface are decomposed into average rigid-body surface motions and residual elastic deformation before the random response analysis is performed. The resulting random response outputs are the random response of the rigid-body motions and the random response of the surface RMS error, which impact the optical performance differently. The structural design changes required to decrease either error is usually quite different. Therefore, it is useful to decompose the total error into its rigid-body and elastic components.

For conventional optics, SigFit will calculate line-of-sight motion in static or dynamic environments. In random analysis, the effect of jitter on MTF can be calculated. This capability for grazing incidence optics is planned for a future release.

9. MONTE CARLO ANALYSIS

A new capability in SigFit is Monte Carlo analyses to allow users to understand the statistics of the optical performance as a function of the statistics of variable factors in the system. As currently implemented in SigFit, the unit variable changes may be represented by FEA result cases due to any perturbation that may be simulated in the FEA. The user specifies the distribution type as normal or uniform, the mean, and the standard deviation of each variable. SigFit performs the desired number of Monte Carlo realizations reporting the statistical results of the rigid-body errors, surface RMS errors, and fitted polynomials.

An example application of a Monte Carlo analysis could be the study of mount variability effects on optical performance. For an optic mounted on three points, unit moments at each mount could be applied as individual load cases. Within SigFit, the user specifies the distribution and uncertainty of the mount moments. SigFit will perform the Monte Carlo analysis and provide the statistics on surface RMS, rigid body motion and polynomial magnitudes. A similar application is to understand the effect of adaptive control actuator resolution by using the influence function predictions as variables. An example is presented below using the optimum actuator layout with 40 actuators presented in Section 6. A resolution of 1.0 mN at each force actuator in the layout was applied with uniform distribution. A Monte

[b] MD Nastran is a registered trademark of MSC.Software Corporation.

Carlo analysis with 1000 realizations was performed to obtain the statistics summary presented in Table 1 and the cumulative probability density shown in Figure 10.

Table 1. Statistical summary of surface RMS of 40actuator adaptive segment due to force actuator resolution.

Surface RMS Statistical Result	Value
Mean	0.065 nm
90% Bound	0.13 nm

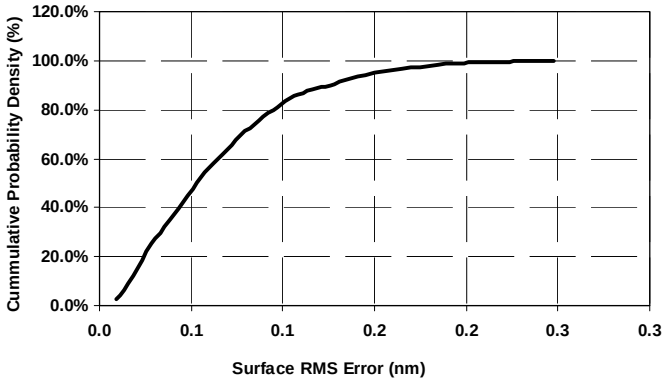

Figure 10. Cumulative probability density vs. surface RMS error for 40-actuator adaptive segment due to force actuator resolution

10. CONCLUSION

Through careful treatment of the nodal displacement predictions from FEA and use of polynomial fitting, the deformations of grazing incidence optical surfaces may be characterized for subsequent optical analysis. Either the Fourier-Legendre or Legendre polynomial set may be chosen based on the system architecture. Future development of this capability will include the employment of array data and power spectral density models to allow characterization of higher frequency deformations as might be caused by local mount effects.

REFERENCES

[1] Elvis, Martin et. al., "Active x-ray optics for Generation-X, the next high resolution x-ray observatory," Proc. SPIE 6266-1K, (2006).
[2] Casey, T. M. Steele, J. M., Brearey, R. R. and Stark, R. A., "A ray tracing technique incorporating finite element analysis for grazing incidence optics," Proc. SPIE 1303-34, (1990).
[3] Genberg, V., Doyle, K. and Michels, G., "An optical interface for MSC Nastran," MSC Conference Proc VPD04-31, (2004).
[4] Michels, G., Genberg, V., and Doyle, K., "Integrating ANSYS mechanical analysis with optical performance analysis with SigFit," ANSYS User Conference Proc., (2008).
[5] Glenn, Paul, "A set of orthonormal surface error descriptors for near cylindrical optics," Opt. Eng. Vol. 23 No. 4, 178-186, (1984).
[6] Doyle, K., Genberg, V., and Michels, G., [Integrated Optomechanical Analysis], SPIE Press, TT 58, (2002).
[7] Michels, G., Genberg, V., Doyle, K., and Bisson, G., "Design optimization of actuator layouts of adaptive optics using a genetic algorithm," Proc. SPIE 5877-22, (2005).
[8] Goldberg, David E., [Genetic Algorithms in Search, Optimization & Machine Learning], Addison Wesley Longman, Inc., Boston, (1989).
[9] Michels, G., Genberg, V., Doyle, K., and Bisson, G., "Design optimization of system level adaptive optical performance," Proc. SPIE 5867-25, (2005).

Appendix A: Low Order Fourier-Legendre Polynomials

(N=axial wave number, M=circumferential wave number)

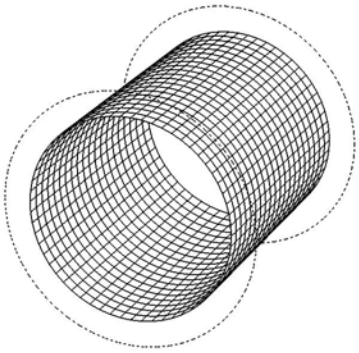

N=0, M=0

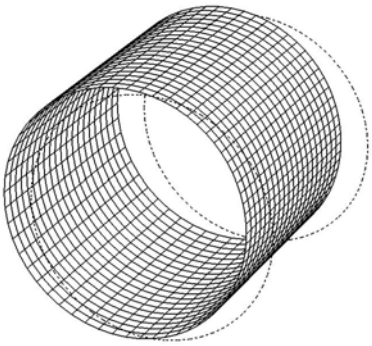

N=0, M=1

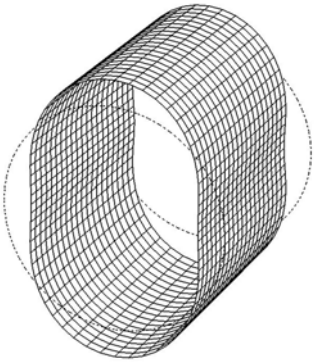

N=0, M=2

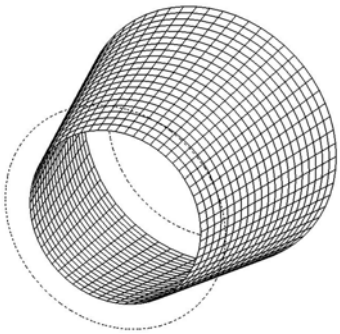

N=1, M=0

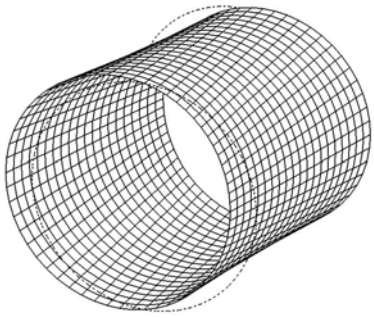

N=1, M=1

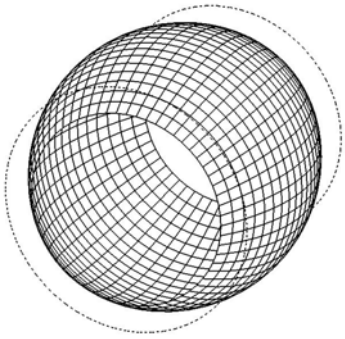

N=2, M=0

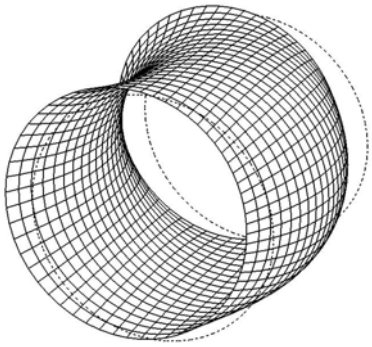

N=2, M=1

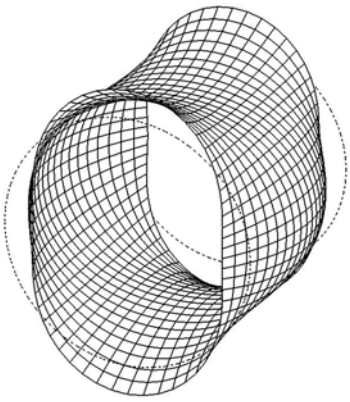

N=2, M=2

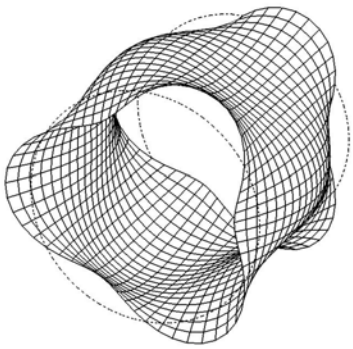

N=2, M=3

Appendix B: Low Order Legendre Polynomials

(N=axial wave number, M=circumferential wave number)

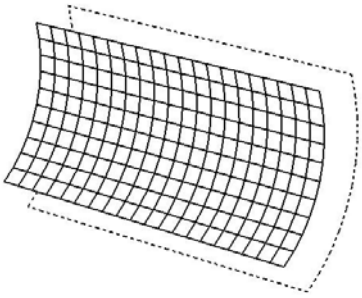

N=0, M=0

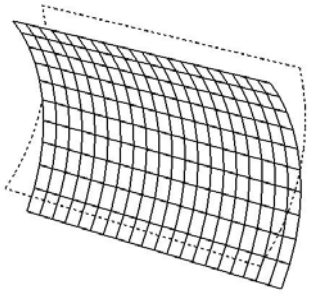

N=0, M=1

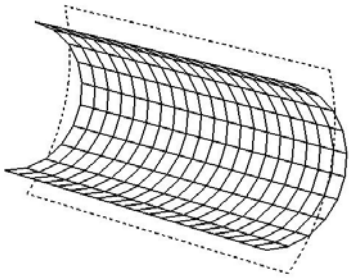

N=0, M=2

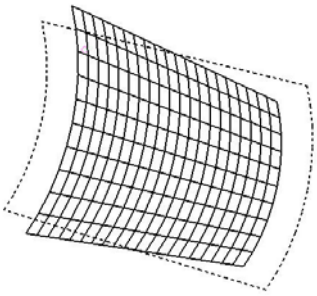

N=1, M=0

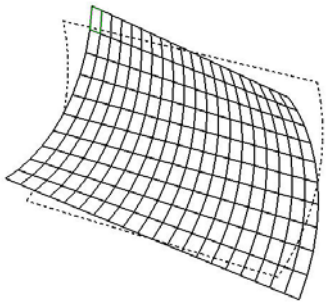

N=1, M=1

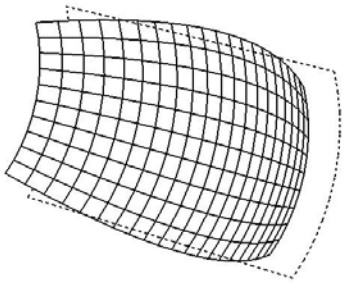

N=2, M=0

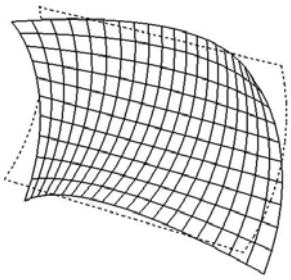

N=2, M=1

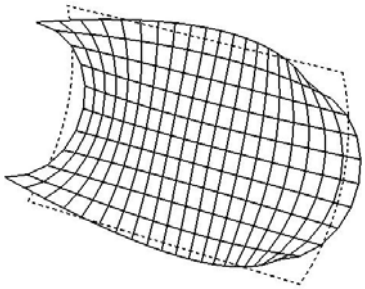

N=2, M=2

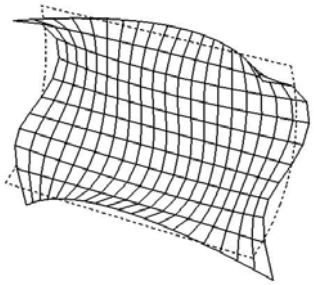

N=2, M=3